Time-of-flight electron spectrometer for a broad range of kinetic energies

Alexander Kothe, Jan Metje, Martin Wilke, Alexandre Moguilevski, Ruba Al-Obaidi, Clemens Richter, Nicholas Engel, Ronny Golnak, Igor Yu. Kiyan, Emad F. Aziz[1, a)]
Joint Ultrafast Dynamics Lab in Solutions and at Interfaces (JULiq)
Helmholtz-Zentrum Berlin für Materialien und Energie (HZB), Albert-Einstein-Str. 15, 12489 Berlin, Germany
and Freie Universität Berlin, FB Physik, Arnimallee 14, 14195 Berlin, Germany

(Dated: 3 December 2012)

A newly constructed time-of-flight electron spectrometer of the magnetic bottle type is characterized for electron detection in a broad range of kinetic energies. The instrument is designed to measure the energy spectra of electrons generated from liquids excited by strong laser fields and photons in the range of extreme ultra violet and soft X-rays. Argon inner shell electrons were recorded to calibrate the spectrometer and investigate its characteristics, such as energy resolution and collection efficiency. Its energy resolution $\Delta E/E$ of 1.6 % allows resolving the Ar 2p spin orbit structure at kinetic energies higher than 100 eV. The collection efficiency is determined and compared to that of the spectrometer in its field-free configuration.

I. INTRODUCTION

Photoelectron spectroscopy constitutes one of the basic experimental methods to study processes initiated by interaction of light with matter. It is widely applied in experiments on photoexcitation of gaseous, solid, and even liquid media. Different techniques are developed to record a spectrum of photoelectrons. These techniques involve, e.g., imaging of photoelectrons by means of their projection onto a position-sensitive detector,[1,2] application of an electrostatic analyzer,[3] and recording the time of flight (TOF) of photoelectrons to a detector placed at a certain distance from the interaction region.[4] Each approach has specific advantages regarding a combination of characteristics such as the electron energy resolution, the collection efficiency, and the capability to resolve the angular distribution of photoelectrons. The kinetic energy range, where some particular requirements for the energy resolution and the collection efficiency need to be satisfied, is determined by the process under investigation. The choice of the type of spectrometer also depends on the geometry and the vacuum conditions of the interaction region. In this work we report on characteristics of a TOF spectrometer designed for experiments with a liquid sample in the form of a free micro-jet. The micro-jet technique was described in Ref.[5] We present the performance of this instrument for a broad range of kinetic energies, extending from a few electron volts (eV) up to nearly 1000 eV. The high-energy limit represents a particular interest for studies where emission of energetic electrons is induced due to interaction of the sample with extreme ultraviolet (XUV) light or with laser radiation of high intensity.[6] To our knowledge, this work represents the first characterization of a TOF spectrometer in the energy range extending to nearly 1000 eV.

TOF electron spectroscopy was applied in a few recent experiments on photoprocesses in a liquid jet.[7,8] To combine a volatile liquid surface in the interaction region with the ultra-high vacuum conditions required for electron detection the TOF region, differential pumping is necessary. This can be achieved by using a skimmer with a small inner diameter as a differential pumping aperture in front of the liquid sample. In the recent experiments[7,8] a skimmer size of a fraction of a millimeter allowed to maintain a difference in the residual gas pressure of several orders of magnitude. In this work we demonstrate that a small skimmer can also be beneficial for the energy resolution of the spectrometer.

In a TOF spectrometer the arrival time of electrons at the detector is equal to L/v, where v and L represent the electron velocity and the path length from the interaction region to the detector, respectively. For a fixed length L, the electron velocity and, consequently, its kinetic energy can be derived from the measured arrival time. Intrinsically, this instrument can be used if photoelectrons are generated by pulsed radiation since the pulse can be used to start the clock. Variations in the path length L for different electron trajectories represent one of the limiting factors of the spectrometer's energy resolution. In order to achieve high resolution, the size of the interaction region should be considerably smaller than the spectrometer length, and the detector acceptance angle should be small as well. The latter significantly reduces the detection rate. The presence of a small skimmer between the liquid sample and the detector can result in additional loss of electrons.

The collection efficiency of photoelectrons can be considerably enhanced by capturing them with a magnetic field, imposed onto the interaction region and pointing toward the detector. The magnetic field bends trajectories of electrons emitted at an angle with respect to the field direction so that the electrons undergo a spiral motion localized around the field axis. If the field is sufficiently strong all electrons of a given kinetic energy, emitted into the half-space on the detector side, can pass through the small skimmer and hit the detector. While the electron kinetic energy is preserved in the presence

[a)] Corresponding author, electronic mail: Emad.Aziz@helmholtz-berlin.de, Emad.Aziz@fu-berlin.de

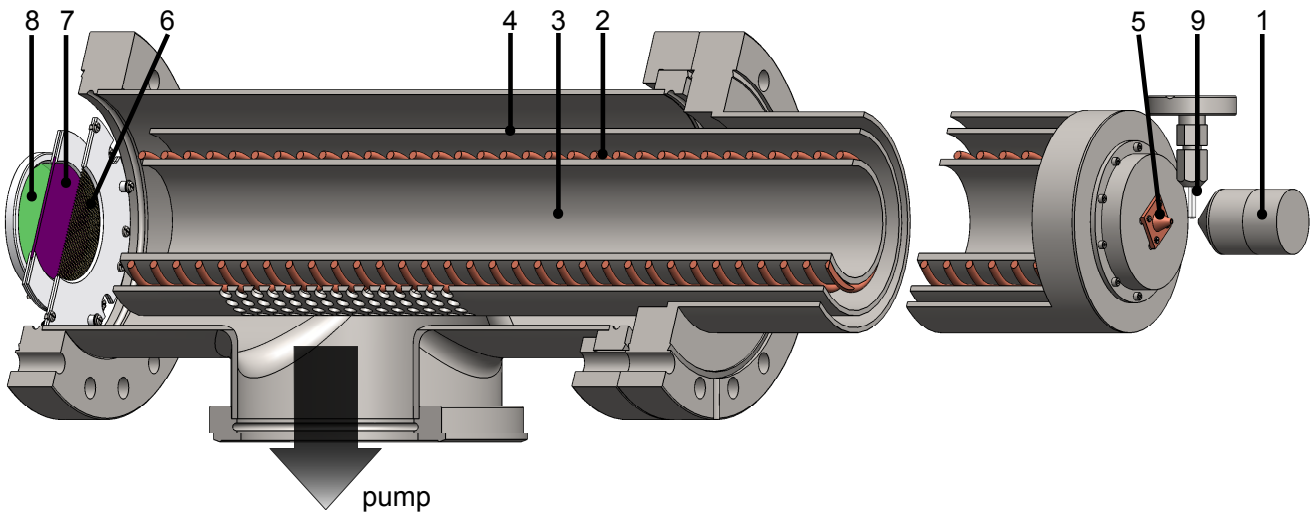

FIG. 1. Design of the TOF electron spectrometer: (1) permanent magnet with a soft iron cone, (2) solenoid, (3) drift tube, (4) μ-metal shield, (5) skimmer of 500 μm size, (6) copper mesh, (7) double-stack of MCP, (8) fluorescence screen, (9) nozzle to introduce the sample.

of a magnetic field, the arrival time to the detector is different for electrons emitted at different angles. This is due to the difference in the length of the corresponding spiral trajectories. In order to preserve the energy resolution, the region of the strong magnetic field should be short compared to the distance to the detector and should be followed by a TOF region with an imposed weak magnetic field. Such a field configuration results in parallelization of electron trajectories in the weak-field region.[4] If the length of this region is large enough so that electrons fly significantly longer than in the region of strong magnetic field, the spread in the arrival time becomes less essential and a sufficiently high energy resolution can be achieved while delivering all the electrons captured by the magnetic field to the detector. Due to the shape of the non-uniform magnetic field lines that resemble a bottleneck, the instrument received the name of "magnetic-bottle TOF spectrometer."

The principles of operation of a magnetic-bottle TOF spectrometer were instructively presented in Ref.[4] including a detailed discussion on factors limiting the energy resolution. Further developments of this instrument are presented in Ref.[9] where the use of a strong permanent magnet was introduced instead of an electromagnet. Following these earlier designs, numerous magnetic-bottle spectrometers were developed in various groups that were modified for the specific requirements of each experiment. A comprehensive analysis of spectrometer characteristics in a kinetic energy range up to a few tens of eV was recently presented in Ref.,[10] where a nearly constant transmission performance was demonstrated. The characterization energy range was extended to approximately 100 eV in Ref.,[11] showing a constant ratio of the energy resolution to the kinetic energy $\Delta E/E$ of 1.6%. In this work we characterize our newly built TOF spectrometer beyond this energy range. In our analysis we compare the performance of the spectrometer with and without application of the magnetic field.

II. DESIGN OF THE SPECTROMETER

The TOF electron spectrometer is designed for experiments on liquids and functional materials in solutions which will be carried out at the newly built High-Harmonic-Generation (HHG) laboratory JULiq and the synchrotron facility BESSY II. The instrument will be used to detect electrons generated under excitation of liquid samples with photons in the energy range of XUV and soft X-rays, which allows to probe the electronic structure of valance and inner shells of compound molecules. It will also be employed to investigate the process of electron emission from solute targets exposed to a strong infrared laser pulse with a peak intensity of up to 10^{16} W/cm^2. Since functional materials in solutions are typically rather diluted samples, enhancement of the collection efficiency of electrons with the use of a magnetic field represents an important issue considered in this work.

The spectrometer design is illustrated schematically in Fig.1. The magnetic bottle is composed by superposition of a strong field B_s created by the permanent magnet (1) and a weak homogeneous field B_w induced in the solenoid (2). The permanent magnet consists of two magnetized cylinders made of Sm_2Co_{17} with a diameter of 25 mm and a length of 15 mm, creating a magnetic field of approximately 500 mT at the flat surface (IBS Magnet, DE2515). A soft iron cone with a 42^o angle to its base and a tip size of 3 mm diameter further increases the field strength in the interaction region located close to the tip. The solenoid coil is made of a Kapton-isolated

copper wire of 0.8 mm thickness, wrapped around the non-magnetizable stainless steel tube (3) with 500 turns per meter. The drift tube has a length of 97 cm and is perforated with holes of 2 mm diameter for pumping purposes (not shown in the figure). A typical coil current of 2 A, generating a magnetic field $B_w \simeq 1.26$ mT inside the drift tube, was used during the tests of the spectrometer. The 2 mm thick μ-metal shield (4) around the solenoid prevents penetration of external magnetic fields into the drift region and, thus, preserves homogeneity of the B_w field and its direction parallel to the spectrometer axis. In order to facilitate pumping of the TOF region, the μ-metal cylinder is perforated with holes of 5 mm diameter in the area facing the turbo-pumps. The skimmer (5) of 500 μm size defines the entrance for electrons into the spectrometer. The distance between the skimmer and the magnet tip was adjusted to 2 mm.

Electrons passing through the drift tube are detected by using a double stack of micro-channel plates (MCPs) (7) with a fluorescence screen (8) mounted behind them. A copper mesh (6) of 88 % transmission in front of the MCPs is used to accelerate electrons before they hit the detector. The mesh is grounded to the drift tube, while an acceleration voltage of +300 V is applied to the front surface of the MCPs. This ensures efficient detection of electrons generated with low kinetic energies. According to the MCPs' characteristics, the gain is nearly constant for electron detection in the energy range from 300 to 1000 V. A voltage of 1500 V is applied across the MCP stack to amplify the electron signal. Amplified electrons are projected onto the fluorescence screen by applying a potential difference of 3000 V between the back MCP surface and the conductive layer of the screen. While fluorescence light, recorded by a CCD camera, is used to visualize the detected electrons, the conductive layer serves as an anode that collects electrons and generates an electric pulse. The pulse signal is decoupled from the high potential of the screen by a capacitor. After amplification, the pulse width generated by a single electron event is in the order of 2 ns. The signal is recorded by a time-to-digital converter card (RoentDek, fADC4) with a bin width of 200 ps. The data acquisition is carried out in the event-counting mode.

III. CALIBRATION PROCEDURE

The calibration and characterization of the spectrometer was performed at the undulator beamline U41-PGM of BESSY II light source at HZB in single-bunch operation mode. The beamline provides horizontally polarized light pulses in the photon energy range from 180 to 1700 eV at a repetition rate of 1.25 MHz. Radiation was loosely focused to a spot of approximately 50 μm size in front of the skimmer of the spectrometer. The spectrometer was attached to the experimental chamber in the horizontal plane so that its axis was collinear to the polarization of the X-rays. The beamline electronics provide trigger pulses at the synchrotron repetition rate, which were used to trigger the converter card. A typical acquisition time of a TOF spectrum accounted two minutes at a sampling rate of up to 40000 events per second.

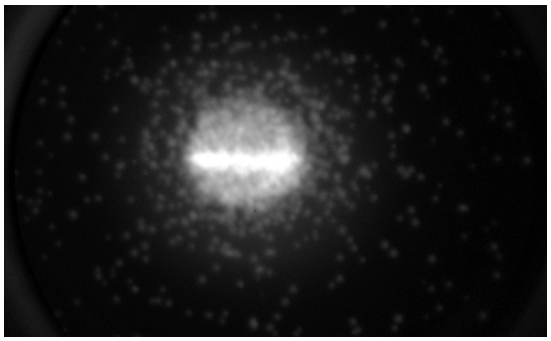

FIG. 2. Image of the fluorescence screen recorded with an exposure time of 100 ms of the CCD camera at a count rate of approximately 20000 events per second.

Argon was used as a sample due to its known electronic structure and ionization cross sections.[12] The gas was fed into the experimental chamber with the use of the microjet setup, designed for future experiments on liquids, and entered the interaction region through a glass nozzle (9) mounted in the vicinity of the skimmer (see Fig. 1). The gas flow was controlled by a dosing valve. A typical pressure of 2×10^{-4} mbar was maintained during the experiment. Small variations in the pressure of less than 2 % over hours ensured basically constant Ar density in the interaction region. Using a skimmer with a 500 μm aperture, a differential pressure of 3×10^{-8} mbar in the TOF region was achieved.

An image of the fluorescence screen recorded by the CCD camera with an exposure time of 100 ms is presented in Fig.2 The image shows a magnified filament of photoelectrons created by the X-ray beam along its propagation direction which is confined by the skimmer aperture. The filament has a thickness of approximately 1 mm on the fluorescence screen, corresponding to a magnification factor $M \simeq 20$. Using the relation $M = (B_s/B_w)^{1/2}$ given in Ref.[4] and taking the value $B_w = 1.26$ mT into account, the magnetic field in the interaction region is estimated to be ~ 500 mT.

The spectrometer calibration was performed by measuring the arrival time of photoelectrons ionized from the $2p$ shell of Ar. This ionization channel has the largest cross section in the photon energy range considered in this work.[13] The $2p$ shell possesses a spin-orbit structure. The ionization potentials related to the $2p_{1/2}$ and $2p_{3/2}$ components of this structure are 250.8 and 248.6 eV, respectively.[14] The high repetition rate of the X-ray pulses restrict the calibration energy range to 4.9 eV and higher. This is because electrons with lower kinetic energies do not arrive at the detector within the time interval of 800 ns between the X-ray pulses, while the converter

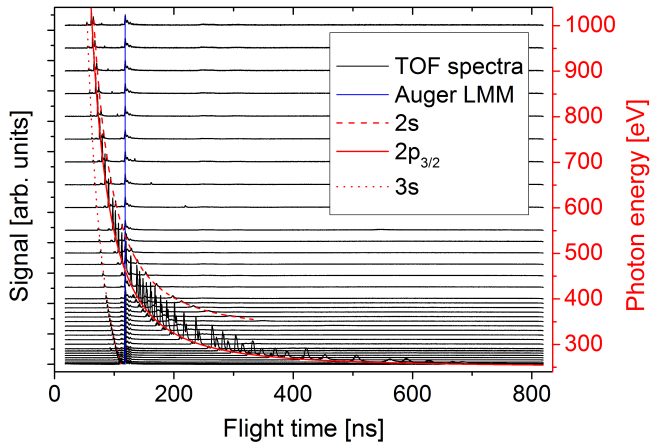

FIG. 3. TOF spectra of Ar (black lines) shifted vertically according to the photon energy (right scale). The Auger LMM peaks are depicted by the vertical blue line. The red curves represent the calibration functions (1) for ionization of the Ar $2s$ (dashed line), $2p_{3/2}$ (solid line) and $3s$ (dotted line) shells.

card already receives the next trigger pulse. Therefore, the lowest photon energy used for calibration was 255.5 eV, which ensured that electrons ionized from both the $2p_{1/2}$ and $2p_{3/2}$ states arrive at the detector within 800 ns after the ionization event.

The calibration data recorded in the photon energy range from 255.5 to 1000 eV are presented in Fig. 3. The TOF spectra are vertically shifted in the figure, whereas the shift of a given trace is proportional to the photon energy used to record the spectrum. The photon energy scale is given by the vertical axis on the right-hand side of the figure, respectively. This facilitates observing the arrival time of electrons, manifested by peaks in the spectra, as a function of the excitation energy. Apart from the peaks associated with ionization of the $2p$ states, the spectra reveal contributions from ionization of the $2s$ and $3s$ shells, as well as from Auger LMM decays of the $2p$ hole. The Auger spectrum is in good agreement with the results presented in Ref.[11] The relation between the electron kinetic energy $E_{\rm kin}$ and the arrival time t measured by the converter card is given by

$$E_{\rm kin} = \frac{m_{\rm e}}{2}\frac{L^2}{(t-t_0)^2}\ , \qquad (1)$$

where $m_{\rm e}$ is the electron mass, L is the path length of electrons from the X-ray focus to the detector, and t_0 accounts for the time offset of the trigger. For a given ionization channel, the kinetic energy is calculated as $E_{\rm kin} = E_{\rm ph} - E_{\rm IP}$, where $E_{\rm ph}$ is the photon energy value provided by the beamline, and $E_{\rm IP}$ is the ionization potential of the initial state. The sequences of the peaks in the TOF spectra associated with ionization of the $2p_{1/2}$ and $2p_{3/2}$ states were fitted to Eq. (1) with the fit parameters L and t_0. The values of their ionization potentials were taken from Ref.[14] The fit result for the $2p_{3/2}$ state is shown in Fig. 3 by the red solid curve. The calibration procedure yielded the value $L = 102$ cm for the distance between the interaction region and the detector.

IV. PERFORMANCE CHARACTERISTICS

The energy resolution and the collection efficiency of photoelectrons represent important characteristics of the spectrometer. Typically an increase of one of these parameters leads to a decrease of another, and it represents a challenging task to achieve high energy resolution simultaneously with high collection efficiency. In this section we consider the performance characteristics of the newly built magnetic-bottle TOF spectrometer. In the analysis we use the performance of the same instrument, but without magnetic bottle, as a reference. In the latter case the permanent magnet was disassembled and a μ-metal shield was mounted around the interaction region. The field-free spectrometer configuration represents the limiting case, where the electron collection is minimal and is solely defined by the cone that comprises straight electron trajectories from the interaction region to the detector. While using the spectrometer without magnetic bottle, a significant improvement in the signal-to-noise ratio was achieved by applying a coil current of the order of 1 A. The induced magnetic field prevented background electrons, originating from surfaces inside the drift tube, from reaching the detector. Though such an unusual field configuration resulted in a slight broadening of the TOF peaks, it had no effect the analysis of characteristics of the magnetic-bottle TOF spectrometer presented below.

A. Energy resolution

The TOF spectra shown in Fig. 3 were transformed from time to energy scale, E, using Eq. (1) with $E = E_{\rm kin}$ and L and t_0 obtained from the fit. The transformation factor $dE/dt \sim E^{3/2}$ was taken into account in these calculations.

The energy resolution, defined by the width of energy peaks, was obtained from Gaussian fits to the energy spectra. The two peaks arising from the Ar(2p) fine structure are well separated in the spectra recorded at low excitation energies and could be fitted to single Gaussian profiles. The individual fits yielded comparable widths for the $2p_{1/2}$ and $2p_{3/2}$ peaks. With the increase of the excitation energy, the fine-structure peaks start overlapping each other. Therefore, at higher kinetic energies the peaks were fitted together to a sum of two Gaussian profiles with equal widths

$$y(E) = A_1 e^{-\left(\frac{E-E_0}{w}\right)^2} + A_2 e^{-\left(\frac{E-E_0-\Delta E_{\rm SO}}{w}\right)^2}\ , \qquad (2)$$

where E_0 denotes the energy position of the $2p_{1/2}$ peak, $\Delta E_{\rm SO} = 2.2$ eV is the energy of the fine structure splitting, w is the Gaussian width of peaks, while A_1 and A_2

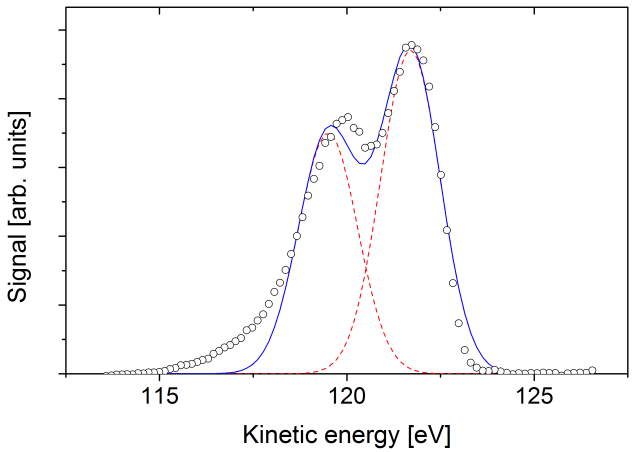

FIG. 4. Energy peaks of the $2p_{1/2}$ and $2p_{3/2}$ electrons generated at a kinetic energy of ~ 120 eV. Solid line represents the fit of Eq. (2) to the experimental spectrum. The individual peak contributions are shown by dashed lines.

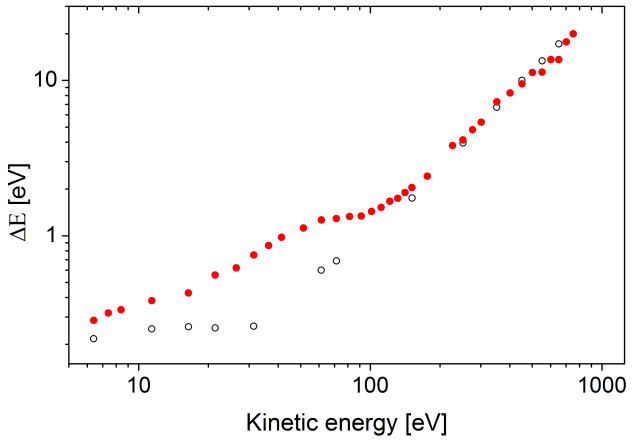

FIG. 5. Energy resolution obtained for the magnetic-bottle (closed circles) and the field-free (open circles) spectrometer configurations.

are their amplitudes, respectively. These four parameters are the fit parameters in the calculations. The Gaussian width w is transformed to a full width at half maximum (FWHM). As an illustration, Fig. 4 shows the results of the fit to a spectrum for which electrons are generated with kinetic energies of approximately 120 eV. In this spectrum the fine structure splitting is still resolved. At kinetic energies higher than 250 eV the $2p_{1/2}$ and $2p_{3/2}$ peaks merge and are not distinguishable.

Photoelectron peaks in the energy spectra are asymmetric, with a steeper slope at the high-energy flank. The peak asymmetry was discussed in detail in Ref.[4] It was shown that a slight displacement of the source of monoenergetic electrons from the magnetic-bottle's axis of symmetry can result in an essential asymmetric broadening of the energy peak, as well as in a change of its position on the energy scale (see Fig. 13 in Ref.[4]). In the present experiment the electron source represents a filament, limited by the skimmer aperture of 500 μm (see Fig. 2), and, therefore, the peak asymmetry is unavoidable. Nevertheless, the fit of Gaussian functions to asymmetric peaks yielded FWHM values which are in good agreement with values obtained from a manual estimation of widths.

Figure 5 shows the energy resolution obtained for both the magnetic-bottle and the field-free spectrometer configurations in the range from 5 to 750 eV. The two curves are displayed on a double logarithmic scale for better visualization of the low energy region. In this region the resolution of the field-free spectrometer is limited due to the coil current used to reduce the background signal. One can see that the resolution obtained with the magnetic-bottle configuration is generally worse at lower kinetic energies. This is due to the collection mechanism leading to a spread in the path length of spiral trajectories, as discussed in the introduction.

The resolution curve obtained for the magnetic-bottle configuration exhibits a short plateau at kinetic energies higher than 50 eV, where the relative resolution $\Delta E/E$ improves. In this region we observe losses in the collection of photoelectrons. With the increase in kinetic energy, electrons emitted at a given angle with respect to the spectrometer axis of symmetry are captured by the magnetic field at a larger distance from this axis. Thus, the electron trajectories become less localized and can be screened by the skimmer. This results in a decrease of the acceptance angle and, simultaneously, in an improvement of the relative energy resolution, which reaches a value of 1.6 % at the kinetic energy of 100 eV. This value is comparable to that of a TOF spectrometer reported in reference.[11] At higher kinetic energies, the collection mechanism becomes even less efficient and the resolution of the magnetic-bottle spectrometer approaches the resolution of the field-free spectrometer. Fig. 5 shows that at energies higher than 200 eV the resolution curves are basically identical. In this range the finite response time of 2 ns of the detection setup to a single event represents the limiting factor for both the field-free and the magnetic-bottle spectrometer configurations. Due to this limitation, $\Delta E/E$ gradually changes from 2 to 2.8 % in the range from 300 to 750 eV.

B. Collection efficiency and acceptance angle

The collection efficiency T is defined by the ratio of the number of detected electrons, S, to the number of electrons generated in the ionization process, Y. Using the electron yield in the $2p$ ionization channel, this quantity is calculated as:

$$T = \frac{S_{2p}}{Y_{2p}} , \qquad (3)$$

where S_{2p} represents the integrated signal of the $2p_{1/2}$ and $2p_{3/2}$ peaks in the energy spectrum, and the ioniza-

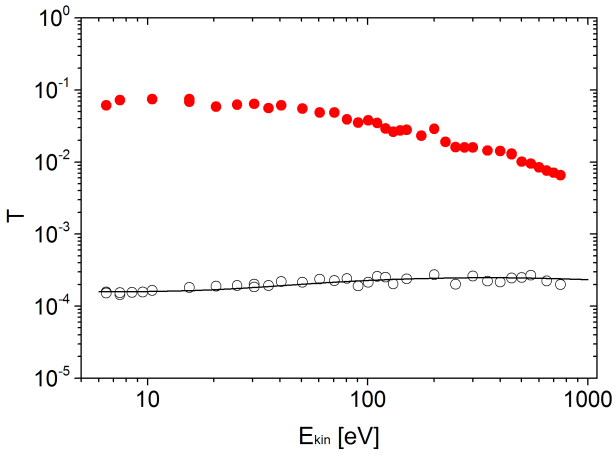

FIG. 6. Collection efficiency of the $2p$ electrons obtained for the magnetic-bottle (red filled circles) and the field-free (black open circles) spectrometer configurations. The solid line represents calculated results for 1.1° acceptance angle by using Eq. (5).

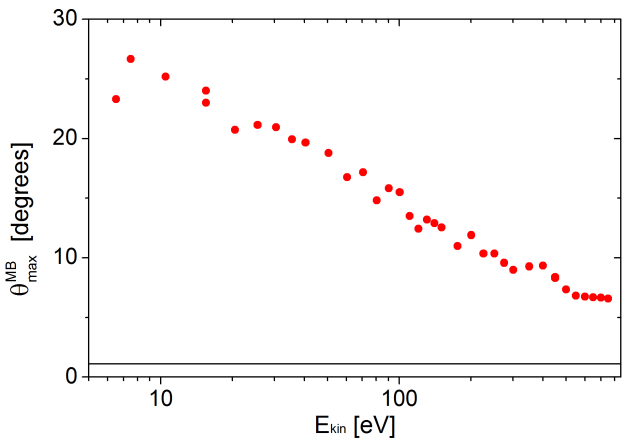

FIG. 7. Dependency of the acceptance angle on the kinetic energies for the magnetic-bottle spectrometer configuration. The acceptance angle of 1.1° of the field-free spectrometer is depicted by a solid line.

tion yield is given by

$$Y_{2p} = \rho_{Ar}\,\Phi\,\tau\,\sigma_{2p}\,D\ . \tag{4}$$

Here ρ_{Ar} is the Ar density, Φ is the flux of X-ray radiation, τ is the acquisition time, σ_{2p} is the partial ionization cross section of the 2p shell, and D is the accepted length of the interaction region along the X-ray beam.

In our analysis we use the fact that the signal in the LMM Auger peaks S_A, arising in the spectra at kinetic energies between 190 and 220 eV, is proportional to the ionization yield Y_{2p}.[11] The kinetic energy of the Auger electrons is independent of the excitation energy and, therefore, their collection efficiency remains unchanged for different photon energies. Hence, by normalizing the S_{2p} signal to the Auger signal S_A recorded in the same spectrum, we obtain the functional dependency of the collection efficiency T on the kinetic energy, though its absolute scale remains undefined.

The absolute value of T can be easily calculated for the field-free configuration since in this case the acceptance angle θ^{FF}_{max} is unambiguously defined by the geometry of the spectrometer. In the present setup $\theta^{FF}_{max} \simeq 1.1°$, determined by the MCP aperture of 40 mm and the distance of 102 cm from the interaction region to the MCP. The absolute value of collection efficiency was obtained by evaluating the integral

$$T = \int_\Omega \frac{1+\beta P_2(\cos(\theta))}{4\pi}\,d\Omega\ . \tag{5}$$

The integrand represents the angular distribution of photoelectrons, expressed in terms of the asymmetry parameter β and the Legendre polynomial $P_2(\cos(\theta))$, and θ denotes the emission angle with respect to the X-ray polarization axis.[15] Since the X-rays are polarized colinear to the spectrometer axis, the integration is carried out over a solid angle Ω limited by a cone with $0 < \theta < \theta^{FF}_{max}$ and $0 < \phi < 2\pi$. The β parameters for ionization of the $2p$ shell of Ar were taken from Ref.[13] The results of these calculations are presented by a solid line in Fig. 6. The energy dependency of T, derived from the experimental data as the ratio S_{2p}/S_A, was multiplied by a constant to obtain the best fit to the calculated value of T in the considered energy range. The results of this normalization are shown in Fig. 6 by open circles, and demonstrate an excellent agreement between the measured and the calculated energy dependencies of T obtained for the field-free spectrometer configuration.

In order to determine the absolute value of T for the magnetic-bottle configuration, we calculated the absolute ratio of collection efficiencies of the magnetic-bottle and the field-free spectrometer configurations at a fixed kinetic energy of 80 eV. In these calculations, recorded at the excitation energy of 330 eV, the S_{2p} signals were first normalized to the measured experimental parameters Φ, τ, and the gas pressure. The absolute ratio of efficiencies was obtained by dividing the normalized signals by each other. The energy dependency of S_{2p}/S_A, obtained for the magnetic-bottle configuration, was then multiplied by a constant in order to match the calculated ratio of efficiencies at $E_{kin} = 80$ eV. The obtained results are shown in Fig. 6 by filled circles. The presented results demonstrate that, with the use of the magnetic bottle, an enhancement by more than two orders of magnitude in the collection efficiency is achieved. This enhancement remains nearly constant up to kinetic energies of 50 eV. At higher energies the magnetic field is not strong enough to catch electrons emitted at larger angles, and the efficiency monotonically decreases by an order of magnitude with the increase of the kinetic energy to 750 eV.

The energy dependency of the acceptance angle for the magnetic-bottle spectrometer, θ^{MB}_{max}, can be obtained by

using Eq. (5) from the data shown in Fig. 6. The results of these calculations are presented in Fig. 7. The acceptance angle monotonically decreases with the increase of the kinetic energy, which results in the loss of photoelectrons, as discussed above. Its maximum value is 25° in the low energy limit which is substantially less than the angle of $\pi/2$ reached in other setups.[4,9] This is due to the screening of electron trajectories by the small skimmer aperture in front of the drift region.

V. SUMMARY

In conclusion, we characterized the performance of a magnetic-bottle TOF spectrometer for a wide range of electron kinetic energies extending up to approximately 1000 eV. With the increase of the kinetic energy, the improvement in the relative resolution $\Delta E/E$ of this instrument is followed by losses in the electron collection. This tendency is shown to be enhanced with the use of a small aperture in front of the drift region. By varying the aperture size, one can achieve a desirable compromise between the collection efficiency and the resolution.

For larger kinetic energies, the arrival time of photoelectrons is decreased and, therefore, the finite response time of the detector to a single event becomes the limiting factor of the resolution. In the present setup, this limitation constitutes the resolution in the energy range above 200 eV, where the magnetic-bottle spectrometer possesses a resolution identical to the field-free spectrometer. However, the collection efficiency of the magnetic-bottle spectrometer is higher by approximately two orders of magnitude at the kinetic energy of 200 eV, and it remains higher by more than one order of magnitude with the increase in the kinetic energy up to 750 eV. This makes the magnetic-bottle spectrometer a superior instrument for electron detection in the high energy limit.

VI. ACKNOWLEDGMENTS

The authors greatly appreciate discussions with B. Winter, U. Hergenhahn, T. Schultz, and members of their groups. This work was supported by the Helmholtz-Gemeinschaft via the VH-NG-635 grant and the extended investment of 2013 (E.F.A.) and the European Research Council grant No. 279344 (E.F.A.).

[1] C. Bordas, F. Paulig, H. Helm, and D. L. Huestis, Rev. Sci. Instrum. **67**, 2257 (1996).
[2] A. T. J. B. Eppink and D. H. Parker, Rev. Sci. Instrum. **68**, 3477 (1997).
[3] S. Hüfner, *Photoelectron Spectroscopy: Principles and Applications* (Springer-Verlag Berlin Heidelberg New York, 2003).
[4] P. Kruit and F. H. Read, J. Phys. E: Sci. Instrum. **16**, 313 (1983).
[5] M. Faubel, B. Steiner, and J. P. Toennies, J. Chem. Phys. **106**, 9013 (1997).
[6] C. I. Moore, J. P. Knauer, and D. D. Meyerhofer, Phys. Rev. Lett. **74**, 2439 (1995).
[7] K. R. Siefermann, Y. Liu, E. Lugovoy, O. Link, M. Faubel, U. Buck, B. Winter, and B. Abel, Nature Chem. **2**, 274 (2010).
[8] F. Buchner, A. Lübcke, N. Heine, and T. Schultz, Rev. Sci. Instrum. **81**, 113107 (2010).
[9] T. Tsuboi, E. Y. Xu, Y. K. Bae, and K. T. Gillen, Rev. Sci. Instrum. **59**, 1357 (1988).
[10] M. Mucke, M. Förstel, T. Lischke, T. Arion, A. M. Bradshaw, and U. Hergenhahn, Rev. Sci. Instrum. **83**, 063106 (2012).
[11] P. Lablanquie, L. Andric, J. Palaudoux, U. Becker, M. Braune, J. Viefhaus, J. Eland, and F. Penent, J. Electron Spectrosc. Relat. Phenom. **156 - 158**, 51 (2007).
[12] U. Becker and D. A. Shirley, *VUV and soft X-ray photoionization* (Plenum Press, New York, 1996).
[13] J. Yeh and I. Lindau, Atomic Data and Nuclear Data Tables **32**, 1 (1985).
[14] A. Knop, H. W. Jochims, A. L. D. Kilcoyne, A. D. Hitchcock, and E. Rühl, Chem. Phys. Lett. **223**, 553 (1994).
[15] S. Hara and M. Nakamura, J. Phys. B: At. Mol. Phys. **19**, L467 (1896).